

Fault-tolerant linear optical quantum computing with small-amplitude coherent states

A. P. Lund,^{1,*} T. C. Ralph,¹ and H. L. Haselgrove^{2,3}

¹*Centre for Quantum Computer Technology, Department of Physics,
University of Queensland, St. Lucia, QLD 4072, Australia*

²*C3I Division, Defence Science and Technology Organisation, Canberra, ACT 2600, Australia*

³*School of Information Technology and Electrical Engineering,
University of New South Wales at ADFA, Canberra 2600 Australia*

Quantum computing using two optical coherent states as qubit basis states has been suggested as an interesting alternative to single photon optical quantum computing with lower physical resource overheads. These proposals have been questioned as a practical way of performing quantum computing in the short term due to the requirement of generating fragile diagonal states with large coherent amplitudes. Here we show that by using a fault-tolerant error correction scheme, one need only use relatively small coherent state amplitudes ($\alpha > 1.2$) to achieve universal quantum computing. We study the effects of small coherent state amplitude and photon loss on fault tolerance within the error correction scheme using a Monte Carlo simulation and show the quantity of resources used for the first level of encoding is orders of magnitude lower than the best known single photon scheme.

Linear optical quantum computing uses off-line resource states, linear optical processing and photon resolving detection to implement universal quantum processing on optical quantum bits (qubits) [1]. This technique avoids a number of serious problems associated with the use of in-line non-linearities for quantum processing including their limited strength, loss, and inevitable distortions of mode shape by the non-linear interaction. The trade-off for adopting the linear approach has been large overheads in resource states and operations. In the standard approach, which we will refer to as LOQC [2], single photons are used as the physical qubits. Although progress has been made in reducing the overheads [3], for fault-tolerant operation they remain very high [4].

An alternative version of linear optical quantum computing, coherent state quantum computing (CSQC) [5], uses coherent states for the qubit basis. This is an unusual approach as the computational basis states are not energy eigenstates and are only approximately orthogonal. Previous work on CSQC has concentrated on the regime where coherent states are relatively large ($\alpha > 2$) and the orthogonality is practically zero. It has been shown that CSQC has resource-efficient gates [6].

In this letter we show how to build non-deterministic CSQC gates for arbitrary amplitude coherent states that are overhead-efficient and (for $\alpha > 1.2$) can be used for fault-tolerant quantum computation. We estimate the fault-tolerant threshold for a situation in which photon loss and gate non-determinism are the dominant sources of error. As our gates operate for any amplitude coherent states, proof of principle experiments are possible using even smaller amplitudes. Given recent experimental progress in generating the required diagonal resource states [7] we suggest that CSQC should be considered a serious contender for optical quantum processing.

For this paper we will use the CSQC qubit basis $|0\rangle = |\alpha\rangle$, $|1\rangle = |-\alpha\rangle$ where $|\alpha\rangle$ describes a coherent state with (real) amplitude α (i.e. $\hat{a}|\alpha\rangle = \alpha|\alpha\rangle$). These

states do not define a standard qubit basis for all α as $\langle -\alpha|\alpha\rangle = e^{-2\alpha^2} \neq 0$, but for $\alpha > 2$ this overlap is practically zero [5]. A general CSQC single-qubit state is

$$N_{\mu,\nu}(\alpha) (\mu|\alpha\rangle + \nu|-\alpha\rangle), \quad (1)$$

where $N_{\mu,\nu}(\alpha)$ normalises the state and depends on the coefficients of the state. A special case is the diagonal states with $\mu = \pm\nu$ which can be written as $|\pm\rangle = N_{1,\pm 1}(\alpha) (|\alpha\rangle \pm |-\alpha\rangle)$. These states form the resource used when constructing CSQC gates using linear optics and photon detection. The diagonal state with a plus (resp. minus) sign has even (odd) symmetry and only contains even (odd) Fock states. This means that a diagonal (i.e. X -basis) measurement can be performed by a photon counter and observing the parity.

The computational or Z -basis measurement is shown in FIG. 1(a) and the Bell state measurement is shown in FIG. 1(b). The Z -basis and Bell state measurements must distinguish between non-orthogonal states. For the measurement to be unambiguous and error free it must have a failure outcome [8]. This occurs in both measurements when no photons are detected. The probability of failure tends to zero as α increases.

A critical part of constructing CSQC gates for all α is teleportation [5, 10]. This is shown in FIG. 1(c). As the teleporter uses unambiguous Bell state measurements there are 5 outcomes to the measurement. Four outcomes correspond to successfully identifying the respective Bell states. When the appropriate Pauli corrections are made the input qubit is successfully transferred to the output. The fifth outcome corresponds to the measurement failure whose probability again decreases to zero as α increases. Upon failure the output of the teleporter is unrelated to the input and hence the qubit is erased. It is this ability to unambiguously teleport the qubit value, in spite of the fact that the basis states are non-orthogonal, that is key to the success of our scheme.

Unitary transformations on a CSQC qubit as defined

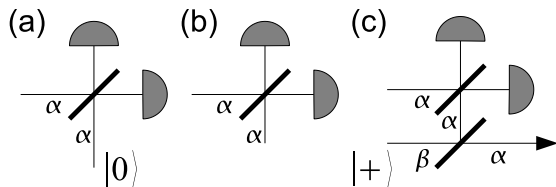


FIG. 1: Schematics for unambiguous CSQC (a) Z -basis and (b) Bell state measurements and (c) CSQC teleportation. Thin lines represent modes whose state is a CSQC qubit with the encoding amplitude shown near each line. The Z -basis measurement in (a) as described in [9] is performed by determining which mode photons are present in. The Bell state measurement in (b) as described in [5] is performed by determining which mode photons are in and how many photons are present. Both these measurements fail when no photons are present. (c) shows how CSQC teleportation [5, 10] is achieved. A Bell state is generated by splitting a $\beta = \sqrt{2}\alpha$ diagonal state on a beam-splitter and performing a Bell state measurement on an unknown qubit and one half of this entanglement. All detectors are photon counters, all beam-splitters are 50:50, and all unlabelled inputs are arbitrary CSQC qubit states.

in Equation (1) will not reach all transformations required to do quantum computing. This is because unitary transformations preserve inner products while various transformations that we might wish to implement (e.g $|\pm\alpha\rangle \rightarrow |\alpha\rangle \pm |-\alpha\rangle$) do not. We implement our gates using non-unitary, measurement-induced gates which act like unitary gates on the *coefficients* of our CSQC qubits for all α . This requires gates which have in general a non-zero probability of failure.

We will construct a universal set of gates based on [5] but applicable for all α , that allows us to implement error correction in a standard way. Our objective is to use the error correction to deal with gate failure errors.

We will choose our universal set of quantum gates as a Pauli X gate, an arbitrary Z rotation (i.e. $Z(\theta) = e^{i\frac{\theta}{2}Z}$), a Hadamard gate and a controlled- Z gate. Each gate acts on the coefficients of the coherent state qubits as they would on orthogonal qubits.

In CSQC the X gate is the only gate deterministic for all α . The gate is performed by introducing a π phase shift on the qubit [5]. The remainder of the gates are implemented via quantum gate teleportation [11]. Just as we are able to implement unambiguous state teleportation, we are able to implement unambiguous gate teleportation. The gates are implemented by altering the form of the entanglement used in the teleporter. The Z rotation is achieved by using the entanglement $e^{i\theta}|\alpha, \alpha\rangle + e^{-i\theta}|-\alpha, -\alpha\rangle$, the Hadamard gate uses the entanglement $|\alpha, \alpha\rangle + |\alpha, -\alpha\rangle + |-\alpha, \alpha\rangle - |-\alpha, -\alpha\rangle$, and the controlled- Z uses the four qubit entanglement

$$|\alpha, \alpha, \alpha, \alpha\rangle + |\alpha, \alpha, -\alpha, -\alpha\rangle + |-\alpha, -\alpha, \alpha, \alpha\rangle - |-\alpha, -\alpha, -\alpha, -\alpha\rangle, \quad (2)$$

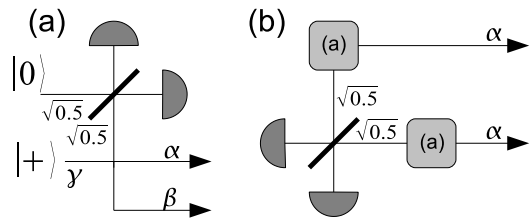


FIG. 2: Schematics for gate entanglement generation. These diagrams have the same layout as those in FIG. 1. (a) shows Z rotation entanglement preparation. A $|+\rangle$ state with amplitude $\gamma = \sqrt{\alpha^2 + \beta^2 + 1/2}$ is split at a three way beam-splitter generating the state $|\alpha', \alpha, \beta\rangle + |-\alpha', -\alpha, -\beta\rangle$ where $\alpha' = 1/\sqrt{2}$ and $\beta = \alpha$ for the rotation. The α' mode is mixed at a beam-splitter with reflectivity $\cos \theta$ with a coherent state of equal amplitude. The two output modes are then detected and the output is accepted if one photon is measured in total (occurring approx. 1:3 times). (b) shows the Hadamard entanglement preparation. Two copies of the entanglement from (a) are used but with different angles θ and θ' and one output mode with coherent state amplitude $\beta = \sqrt{1/2}$. Next, one β mode from each state are combined at a beam-splitter with reflectivity $\cos \delta$ and the output modes are detected. The generation succeeds when only one photon is detected in total. If we choose the rotation angles as $\theta = 3\pi/4, \theta' = \pi/4, \delta = \pi/4$ and perform an X correction on one of the modes the desired entanglement is produced. On average this procedure succeeds approx. 1:27 times.

which is used as the shared entanglement of two teleporters. The controlled- Z entanglement can be generated from the Hadamard entanglement with coherent state amplitude $\sqrt{2}\alpha$ by splitting the outputs at 50:50 beam-splitters. The procedures to generate the Hadamard and Z -rotation entanglement are shown in FIG. 2.

Depending on the outcome of the Bell state measurement in a teleported gate, it may be necessary to apply an X and/or Z Pauli operator to the output. In this paper, we assume that these Pauli operators are not applied directly, but rather absorbed into the error-correction process via the *Pauli frame* technique [12]. If the outcome of the Bell state measurement is failure, then we say the gate failed and the qubit on which it acted upon is erased.

In calculating a noise threshold for CSQC it is necessary to establish a model for the noise experienced by each operation (i.e. gates, measurements, and preparations). This model is expressed in terms of two parameters: the qubit amplitude α , and a loss parameter η (see below). We use this model to simulate concatenated fault-tolerant error-correction protocols. A particular setting of the parameters (α, η) is said to be *below the threshold* if the rate of uncorrectable errors is observed to decrease to zero as more levels of error correction are applied. Here we calculate the *threshold curve*, defined to be the curve through the α - η plane which lies at the boundary between the sets of parameters that are above and below the threshold.

An important feature of our noise model is the inclusion of two types of error: *unlocated* and *located* errors. A located error occurs when a gate fails. The experimenter has knowledge about when and where these errors occur. Unlocated errors are caused by photon loss as these errors are not directly observable. Given that our noise model includes both unlocated and located errors, we use an error-correction protocol which has been designed to deal effectively with combinations of these two error types. We have chosen to utilise the “circuit-based telecorrector protocol” described in [4]. This protocol uses error-location information during ancilla-preparation and syndrome-decoding routines, thus achieving a high tolerance to located noise, whilst achieving a tolerance to unlocated noise similar to that of standard protocols [13, 14].

In practice, other noise sources would be present. Two examples are mode mismatch and phase mismatch. These noise sources will generate additional unlocated and located errors in the teleported gates. The effect of these errors will be similar to those in our simplified noise model. Depending on their strength, they may have a significant effect on the noise threshold curve. We note that these errors are *systematic*, and in principle can be greatly reduced by using appropriate locking techniques.

The probability of gate failure varies as a function of the input qubit state. For simplicity in the simulations, we apply the worst-case probability value, which corresponds to the input state $|+\rangle$. The maximum probability of failure (per qubit) for Z -basis measurements, and Clifford group operations [15] implemented by gate teleportation is equal to

$$q = \frac{2}{1 + e^{2\alpha'^2}}. \quad (3)$$

In this equation $\alpha' = (1-\eta)\alpha$ is an effective encoding amplitude which incorporates the effects of loss. In the case of the controlled- Z gate, this failure probability applies independently to each of the two qubits. Upon a gate failure the input qubit is erased. For simplicity we model this effect by completely depolarising the qubit upon a located error occurring.

We model photon loss by assuming that each optical component, each detector and each input coupling causes some fraction of the input intensity to be lost, and that this loss is equal for all modes. Due to the properties of a linear network with loss it is possible to assign one effective input coupling loss which incorporates all of this loss together. We also assume that the output of each gate includes the loss due to the detectors from the *next* gate or measurement. From this we can assign an effective input loss rate η which combines the *detector, component and input* efficiencies together incorporating all these effects.

The effect of loss on a CSQC qubit is to induce a random Z operation and decrease the coherent state amplitude [16]. We assume that the decrease in amplitude is

TABLE I: Error rates for the models used to calculate the threshold curve for CSQC. The coefficients in the H -gate and C - Z gate arise from the larger α required for generating the entanglement and are worse case. Two models for qubit storage are considered as shown in the row labelled “Memory”. In one model we consider no noise in the operations that store CSQC qubits and the second we introduce photon loss into these operations at the same rate as introduced by the gates.

	Loc. errors	Unloc. X error	Unloc. Z error
Memory	0	0	p or 0
H-gate	q	$1.6p$	$1.6p$
C - Z gate	q	0	$2.5p$
$ +\rangle$	0	0	p
X -meas	0	0	0

compensated by changing the amplitudes of the coherent states in the entanglement used for the teleported gates. The probability of Z error on a diagonal CSQC state is

$$p = \frac{1}{2} \left(1 + \frac{\sinh(2\eta - 1)\alpha^2}{\sinh \alpha^2} \right) \quad (4)$$

where η is the overall fractional loss as defined above.

In the Z rotation and the controlled- Z gates, photon loss causes a Z error on the output state. These are due to the loss in the diagonal states from the generation of the entanglement. In the Hadamard gate, there are two diagonal states required and a loss in one induces a X error on the output and a loss on the other induces a Z error on the output (these errors are uncorrelated).

In our analysis we consider two noise models which are summarised in TABLE I. We are considering here an error-correction protocol which consists of several levels of concatenation. The noise model in TABLE I applies only to the lowest level of concatenation (that is, to error-correction circuits that are built using unencoded “physical” gates). For all higher levels of concatenation, we assume a noise model identical to that considered in [4] for the “circuit-based telecorrection protocol”, since the arguments used to derive that noise model are applicable to our situation. Thus, our noise model and error-correction protocol are identical to that of [4] for concatenation levels 2 and higher, and so we do not perform new simulations for these concatenation levels. Instead, we directly utilise the best-fit polynomials that were obtained in [4], in order to model the mapping between noise rates and effective noise rates for all concatenation levels other than the first.

For the first level of concatenation, we perform new numerical simulations, for the noise models in TABLE I. The simulator was a modified version of the one used in [4]. All controlled-NOT gates were replaced by controlled- Z gates and two Hadamard gates and simplifications of this circuit were performed. Separate simulations were performed for protocols based on the 7-qubit

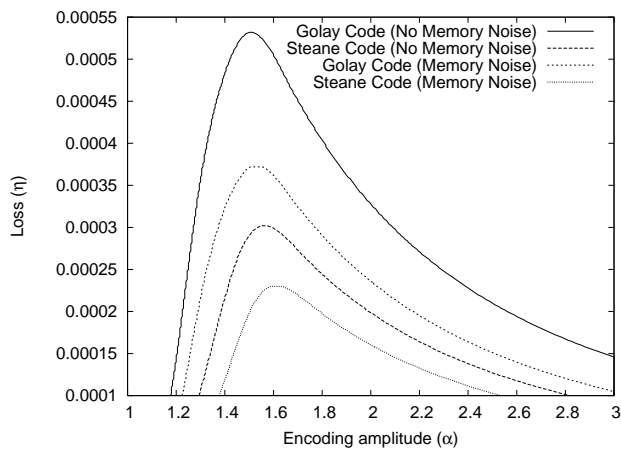


FIG. 3: Thresholds for CSQC using the 7 qubit Steane and 23 qubit Golay code for both memory noise models.

TABLE II: Effective error rates and resource usage for the 7-qubit Steane code with memory noise enabled. Coherent state amplitude used for this table is $\alpha = 1.56$ and loss rate $\eta = 4 \times 10^{-4}$. This corresponds to gate error rates in our model of $(p, q) = (2 \times 10^{-4}, 0.015)$. Resource usage is defined to be the total number of gates, preparations, measurements, and quantum memories used. Resource are used in the following fractions for all levels of concatenation: Memory 0.284, Hadamard 0.098, controlled-Z 0.343, Diagonal states 0.164, X-basis measurements 0.111. Also shown is an estimate of the maximum length of computation possible assuming the entire computation succeeds with probability 1/2.

LEVEL	Unloc. rate	Loc. rate	Max. comp. steps	Resource usage
1	4×10^{-4}	8×10^{-3}	82	1.0×10^3
2	1.7×10^{-4}	2×10^{-3}	3.3×10^2	8.7×10^5
3	2.8×10^{-5}	2.1×10^{-4}	3.0×10^3	4.5×10^8
4	7.4×10^{-7}	3.6×10^{-6}	1.6×10^5	2.1×10^{11}
5	5.3×10^{-10}	1.7×10^{-9}	3.1×10^8	9.6×10^{13}

Steane code and the 23-qubit Golay code. The resulting threshold curves are shown in FIG. 3. An interesting feature is that *increasing α beyond a certain point causes a reduced tolerance to photon loss.*

TABLE II estimates the resource-usage for one round of error-correction, for 5 levels of concatenation. An advantage of CSQC over LOQC is lower resource usage. Using TABLE II and the success probabilities in Fig. 2 we find that CSQC consumes approximately 10^4 diagonal resource states per error correction round at the first level of concatenation. This is 4 orders of magnitude less than the number of Bell pair resource states consumed under equivalent conditions by the most efficient known LOQC scheme [4]. However, there is a trade-off. The photon loss threshold we find for CSQC is an order of magnitude smaller than that for LOQC. This means

that if the loss budget is too large then CSQC may not be scalable or may require so many levels of concatenation that the resource advantage is lost. We note that the physical resources in terms of specific optical states required to implement CSQC and LOQC are different. Nevertheless we believe comparing resource state counts still gives a good estimate of the relative complexity of the two schemes. In future work, it would be valuable to include other sources of noise and improve upon some of the pessimistic assumptions made in deriving the noise model. One could consider ways of optimising the fault-tolerant protocol in order to take advantage of the relative abundance of Z -errors compared with X errors.

We have shown how to construct a universal set of gates for coherent state quantum computing for any coherent state amplitude. Provided the coherent state amplitudes are not too small ($\alpha > 1.2$) and photon loss is not too large ($\eta < 5 \times 10^{-4}$) it is possible to produce a scalable system. To our knowledge this is the first estimation of a fault-tolerance threshold for non-orthogonal qubits. As our gates work for all values of α , proof of principle experiments are possible using already demonstrated technology.

We acknowledge the support of the Australian Research Council, Queensland State Government and the Disruptive Technologies Office.

* Electronic address: lund@physics.uq.edu.au

- [1] P. Kok, *et al.* Reviews of Modern Physics, **79** 135 (2007).
- [2] E. Knill, *et al.* Nature (London) **409**, 46 (2001).
- [3] M. A. Nielsen, Phys. Rev. Lett. **93**, 040503 (2004); D. E. Browne and T. Rudolph, Phys. Rev. Lett. **95**, 010501 (2005); T. C. Ralph, *et al.*, Phys. Rev. Lett. **95**, 100501 (2005).
- [4] C. M. Dawson, *et al.*, Phys. Rev. A, **73**, 052306 (2006).
- [5] T. C. Ralph, *et al.*, Phys. Rev. A, **68**, 042319 (2003).
- [6] H. Jeong and T.C.Ralph, *Quantum Information with Continuous Variables of Atoms and Light*, Ed. N.Cerf (2007) quant-ph/0509137.
- [7] A. Ourjoumtsev, *et al.*, Science, bf 312 83 (2006); J. S. Neergaard-Nielsen, *et al.*, Phys. Rev. Lett. **97**, 083604 (2006); K. Wakui, *et al.*, quant-ph/0609153 (2006).
- [8] I. D. Ivanovic, Phys. Lett. A **123**, 257 (1987).
- [9] H. Jeong and M. S. Kim, Phys. Rev. A, **65** 042305 (2002).
- [10] C. H. Bennett, *et al.*, Phys. Rev. Lett., **70**, 1895 (1993).
- [11] M. A. Nielsen and I. L. Chuang, Phys. Rev. Lett., **79**, 321-324 (1997).
- [12] E. Knill, Nature, 434:39-44 (2005).
- [13] A. M. Steane, Phys. Rev. A, 54:4741 (1996).
- [14] B. W. Reichardt, quant-ph/0406025 (2004).
- [15] Non-Clifford group operations need not be implemented deterministically in the physical gates. They are only needed to generate an offline resource state to implement their operation in a fault-tolerant manner (see M. A. Nielsen and I. L. Chuang, *Quantum Computation and Quantum Information*, CUP (2000) Chapter 10).

- [16] S. Glancy, *et al.*, *Phys. Rev. A* **70**, 022317 (2004).
- [17] D. Aharonov and M. Ben-Or, *STOC '97: Proceedings of the twenty-ninth annual ACM symposium on Theory of computing*, p176–188, (1997).